# Authors' Response to Reviewers' Comments

August 4, 2024

---

**Title**: Millimeter-Wave Resonant Beam SWIPT

**Author**: Shuaifan Xia, Qingwei Jiang, Wen Fang, Qingwen Liu, Shengli Zhou, Mingqing Liu, and Mingliang Xiong

**Manuscript ID**: IoT-38060-2024

---

We would like to thank the Editor and the anonymous reviewers for their constructive feedback on the original submission, which contributed to an improved revised manuscript.

Please note that the changed or added sentences are colored blue in the revised manuscript.

**Remark**. Unless otherwise stated, all equations, figures, citations, remarks, and (sub-)sections are referenced with respect to the numbering used in the *revised* manuscript.

## Response to Editor

*"This paper considered a millimeter wave resonant beam system for SWIPT (mmRB-SWIPT) by leveraging retro directive antenna arrays to enable automatic beam alignment and enhanced transmission efficiency. The reviewers have concerns regarding the realistic application of the proposed architecture, the guarantee of transmission distance, the decoding process, the discussions on the effectiveness of multi-device scenarios, the discussions on the tradeoff between energy harvesting and information transmission, the hazardous issues on human beings, and the simulation results. Besides, there are a few minor issues to be aware of. The authors are suggested to carefully answer the reviewers' comments and revise the paper accordingly. "*

**Response.** Thanks for your time and effort in this manuscript. Following your advice, we carefully studied every comment of the reviewers in an attempt to improve the academic content of this submission.

We have addressed the itemized comments from reviewers in the revised version as follows. Your dedication to the editorial process is deeply respected, and we are truly thankful for the positive influence it has had on our work.

## Response to Reviewer 1

*"This paper investigates the SWIPT using resonant beam in the mmWave wavelength. In general, this work is the extension of the author previous works on optical spectrum, to another frequency band with directional transmission. Although this work is solid, this paper needs the following revision before acceptance."*

**Response.** Thanks for recognizing the contributions and the positive assessment of our submission. We have investigated the SWIPT via optics previously and tried to extend our model and structure to mmWave in this manuscript. We would like to express our gratitude for the time and effort you have dedicated to reviewing our manuscript.

Following your suggestions, we have revised the manuscript carefully. Your comments have been addressed in the revised version as follows.

R1.1 *"For resonance, the transmission distance needs to be multiples of the half wavelength of the transmission frequency. Although it is much easier in the mmWave than in optical wavelength, the authors still need to how to realize/guarantee it."*

**Response.** Thank you for your constructive comment. Indeed, the transmission distance should be integer multiples of wavelength to maintain the stable resonance. In our proposed system, this requirement still applies and is satisfied.

Theoretically, to establish the resonance, the transmission distance should be integer multiple(s) of wavelength to induce the constructive interference. This is especially true in the theoretical analysis where the wavelength and frequency of the carrier wave is fixed to a specific value. In practice, however, the resonance can be established even with displacement of transceivers. The phenomenon can be attributed to the fact that as the distance changes, the frequency of the wave would drift accordingly, satisfying the wavelength requirement constantly.

In our previous works on the optical resonant beam system (RBS), real-world experiments have validated this point [1, 2]. In the context of laser resonator, the gain medium is not fixated on a specific frequency but allows a range of frequencies. When the distance changes, the frequency would drift accordingly and is amplified by the gain medium, forming a stable resonance.

In this manuscript, mmWave is adopted as the carrier wave for power and information transmission. In our setup, the mmWave signal is transmitted back and forth to form the stable resonance. Being similar to the light wave, the frequency of mmWave can drift around the central frequency when the transmission distance changes. The phase-locked loop adopted in our system also supports a range of frequency. Also, during the establishment of the resonance, the frequency of the signal would also

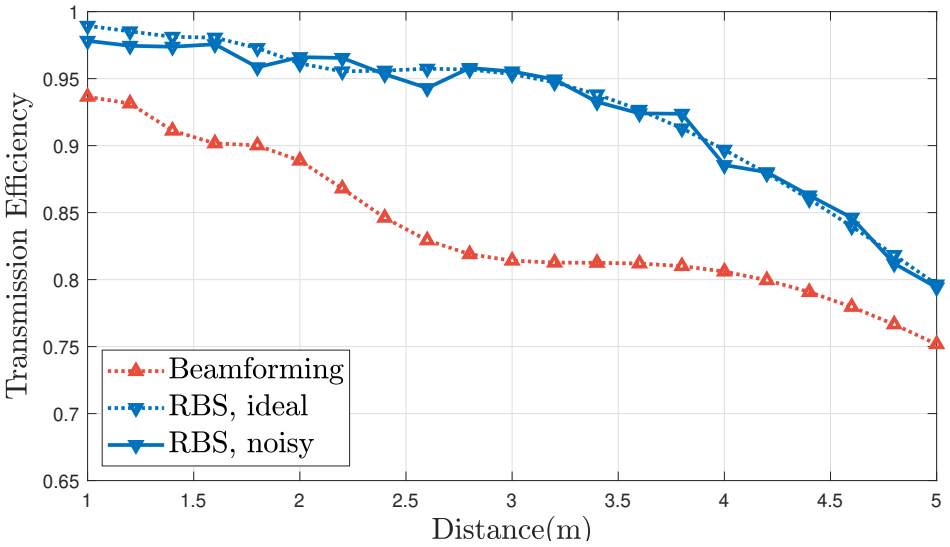


Figure R.1: Transmission efficiency with different distances.

self-adaptively drift in accordance with the transmission distance, and finally meet the wavelength requirement to reach a stable resonance.

Our simulation results have also testified this point. In Fig. R.1, we could see that as the distance increases, the transmission efficiency is not affected by the wavelength requirement. This means that the resonance can be established as long as the transmission distance does not exceed the maximum allowed range. As for the wavelength, the frequency of the wave can drift around its center to meet the criterion.

We once again thank you for your constructive suggestion, following which we have revised the manuscript to elaborate on the resonance criterion. The supplemented detail can also be found in Sec. III. B of the revised version in blue color.

With both BS and UD equipped with retro-directive antenna arrays, the power flows bidirectionally. During each iteration, the phases of antenna elements undergo refinement, reducing the disparity between the received electric field across two consecutive iterations, ultimately converging to a negligible value. Subsequently, the distribution stabilizes and is repeatedly produced in further iterations. The stabilized power distribution is described as *self-reproducing*.

The establishment of a stable resonance requires that the transmission distance to be integer multiples of wavelength. In the initialization process, the signal with a certain bandwidth is transmitted. The actual frequency of the signal would drift around its central frequency to

adapt the transmission distance, and finally reach a stability to meet the wavelength criterion in accordance with the actual transmission distance.

R1.2 *"On the tradeoff between energy and information transmission, the authors need to discuss more. Currently, Section V. B. is not sufficient. More analytical expression on the tradeoffs with some numerical results are needed."*

**Response.** We greatly appreciate your kind and helpful comments. The trade-off between power and information transfer is indeed a typical issue of SWIPT systems. This issue is more complex in our system due to the resonance mechanism.

In our system, the power on the user device's (UD) side is split into three parts: i) charging the UD, ii) retrieving downlink information, iii) being returned to BS, where the uplink information is modulated with the third part. This has leads to a triangular relationship among the power for charging $P_{\text{charge}}$, the power for downlink communication $P_{\text{comm}}$, and the power for uplink communication $P'_{\text{comm}}$. Counter-intuitively, if we increase the ratio of power that is returned from the UD, $P_{\text{charge}}$ would also increase after the stable resonance is obtained. This can be attributed to the resonance mechanism underlying. If more power is returned (feedback) into the resonance, the base station (BS) would have more power to amplify, thus increase the power over-the-air for the stable resonance. Moreover, the returning ratio is limited below a certain threshold to avoid over-amplification, where each of the power amplifiers on the BS works in saturation state hampering the overall efficiency and the retro-directivity.

Following your helpful suggestion, we have added more discussion supported by numerical results in Sec. V. The supplemented information can be found in the revised version of our manuscript in blue color, and is also attached below.

**Power Splitting Ratio**

The power splitting ratio for signal processing, power harvest, and information retrieving is of great significance. The power received by the UD is splitted into three part: i) energy harvest, ii) information retrieval, and iii) return to BS. To avoid ambiguity, we adopt the

following notations for further discussion.

$$\begin{cases} P_{\text{return}} = \alpha P_{\text{R}} \\ P_{\text{charge}} = \beta P_{\text{R}} \\ P_{\text{comm}} = \gamma P_{\text{R}} \\ \alpha + \beta + \gamma = 1 \end{cases}, \tag{1}$$

where $P_{\text{R}}$ is the total power received by UD, $P_{\text{return}}$, $P_{\text{charge}}$, and $P_{\text{comm}}$ denote the power for return, energy harvest, and downlink communication respectively.

The optimal solution for UD is to maximize the power available for charging as well as return adequate power for the uplink information carrier. In Fig. 13., the downlink power is above 20 dBm even with a transmission distance at 5 m. With $\gamma = 0.6\%$, we have the downlink communication power $P_{\text{comm}} \approx 2$ dBm, which is well adequate for wireless communication.

However, for the uplink communication, there is a trade-off between the communication and power harvest. The BS is designed to divide a part of the returned power to retrieve the uplink information, in our configuration, the ratio is $10\gamma$. The power available for uplink communication can be put as:

$$P'_{\text{comm}} \leq 10\alpha\gamma P_{\text{R}}. \tag{2}$$

The inequality accounts for the over-the-air transmission loss on the uplink. Intuitively, if we increase the value of $\alpha$, we could have more power available for uplink communication, but less power for the UD to harvest. However, the numerical simulation has suggested a counter-intuitive conclusion, i.e., increasing $\alpha$ will lead to more power available for charging the UD. This is due to the resonance principle, as the returned power increases, the system is stimulated to operate with higher power. The results with different $\alpha$ values are outlined in the table below.

| $\alpha$ | **Charging Power** (dBm) | **Downlink Comm. Power** (dBm) | **Uplink Comm. Power** (dBm) |
|---|---|---|---|
| 0.2% | 18.982 | −3.202 | −20.608 |
| 0.3% | 26.204 | 4.025 | −11.781 |
| 0.4% | 35.224 | 13.049 | −1.445 |

Moreover, the return ratio $\alpha$ also has impact on the efficiency of the system. Excessively high $\alpha$ may force the power amplifiers to a saturation state, thus reducing the overal efficiency and prolong the initialization of stable resonance. The maximum allowed value for $\alpha$ may

vary depending on the configuration of antenna and other components. With our current parameters, the $\alpha$ is limited below 0.5%. If the returned power is excessively high, the system will be pushed to a saturated state where every power amplifier works in saturation state, resulting in decline of overall efficiency and negative impact on the retro-directivity.

R1.3 *"The hazardous issues on human beings also need to be discussed. This may also lead to the maximum transmission power limit and radiation pattern optimization. "*

**Response.** Thank you for your insightful comment. Radiation safety is indeed of great importance for the proposed system, especially concerning its practical application. Following your advice, we have investigated the potential hazardous issues of the system and supplemented a discussion in Sec. V. The discussion is detailed in Sec. V. C of the revised manuscript and is highlighted in blue color. The supplemented subsection is also attached below.

While this manuscript represents our first attempt to extend our work to the mmWave spectrum, we have previously conducted comprehensive analyses regarding the safety concerns of the optical system. A key feature of the RBS is its intrinsic safety mechanism, where the system halts automatically when a foreign object enters the power zone. This occurs because the power loss due to obstruction exceeds the system's operational threshold. Similarly, mmWave signals are easily absorbed by human bodies. If a human enters the power zone, significant power loss is induced, interrupting the resonance. The system cannot re-initiate resonance as the power loss surpasses the power amplifier's compensation capacity. The logic is identical across different spectra since they can both be absorbed/obstructed. Therefore, the proposed mmWave RBS also features intrinsic safety similar to the optical system.

We are actively planning to undertake a comprehensive analysis regarding the safety issues of the proposed mmWave RBS to ensure its practical viability. Please follow our future publications if the RBS continues to be of research interest to you.

### Radiation Hazard and Safety Concerns

In practical application, the radiation hazard of wireless systems is of great concerns. In this paper, the proposed system employs mmWave as the spatial carrier of power and information. The main safety concern over mmWave radiation is the heat absorbed by eyes and skins since the radiation is non-ionizing [3, 4]. To assess the radiation of signals with frequency range from 10 GHz to 300 GHz, the power density is adopted as the main measurement, with $\mathrm{W/m^2}$ as the unit [4]. A guideline from the International Commission on Non-Ionizing Radiation Protection

(ICNIRP) suggested a power density of 200 W/m$^2$ averaged over 6 minutes and a square 4 cm$^2$ surface area as the local exposure threshold for EM fields in this frequency range [5].

Being different from the traditional wireless power transmitter that continuously emits power, the BS in our proposed system requires the resonant feedback from UD to amplify and emit the power beam, thus maintaining the resonance. In the case where human body obstructs the resonant beam, the power lost over the air (OTA) would increase drastically, resulting in the resonance being cut off. Referring to (20), $\xi$ is the power gained from amplification process, of which the maximum possible value is determined by the power amplifier. During the human invasion, the transmission efficiencies of both downlink and uplink drop significantly, leading to a large $\epsilon$. Once the power lost exceed the maximum allowed power gain, i.e., $\epsilon > \xi$, the resonance is destroyed automatically. The resonance cannot be re-initiate before the obstruction is cleared. Therefore, the only radiation cast on the invading object is the portion of power that is already OTA, the radiation is instantaneous instead of continuous.

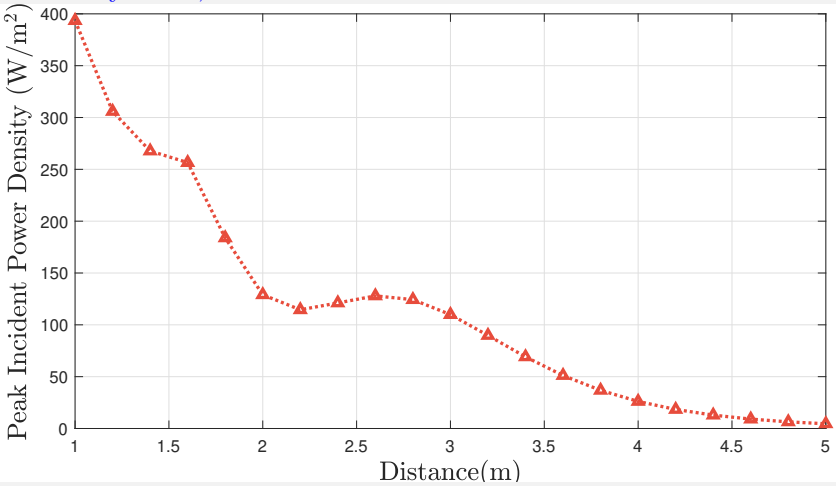


Figure R.2: Instantaneous peak power density incident on the invading object.

A preliminary simulation is conducted supposing the invading object obstructs the beam completely. The instantaneous peak power density incident on the invading object is depicted in Fig. R.2. The $x$-axis of Fig. R.2 is the distance between BS and UD of the system. The obstacle is set to have a constant distance of 0.5 m from the BS. In the small distance setup, the peak power density seems to exceed the maximum allowed by the guidline. However, since the resonance is immediately cut off after invasion, the object will not be radiated continuously. If the power density is averaged over a time span of 6 minutes according to the ICNIRP guideline, the exposure level is reduced to a negligible order of $10^{-6}$ W/m$^2$ since the power radiation is

relaxed within 1 $\mu$s.

Obstacle invasion to the resonance has also been studied in the realm of the optical RBS. The inherent safety feature of the RBS is comprehensively examined in [6], where analytical models are established to investigate the electromagnetic behavior of the system during the invasion.

We would like to express our gratitude again for your time and effort spent reviewing our submission. Your suggestions have been very helpful for us to improve our work.

## References


[1] W. Wang, Q. Zhang, H. Lin, M. Liu, X. Liang and Q. Liu, "Wireless Energy Transmission Channel Modeling in Resonant Beam Charging for IoT Devices," *IEEE Internet of Things Journal*, vol. 6, no. 2, pp. 3976-3986, April 2019.

[2] Q. Liu, M. Xiong, M. Liu, Q. Jiang, W. Fang and Y. Bai, "Charging a Smartphone Over the Air: The Resonant Beam Charging Method," *IEEE Internet of Things Journal*, vol. 9, no. 15, pp. 13876-13885, 1 Aug.1, 2022.

[3] T. Wu, T. S. Rappaport and C. M. Collins, "The human body and millimeter-wave wireless communication systems: Interactions and implications," in *2015 IEEE International Conference on Communications (ICC)*, London, UK, 2015, pp. 2423-2429.

[4] R. Dilli, "Implications of mmWave Radiation on Human Health: State of the Art Threshold Levels," *IEEE Access*, vol. 9, pp. 13009-13021, 2021.

[5] I. C. on Non-Ionizing Radiation Protection *et al.*, "Guidelines for limiting exposure to electromagnetic fields (100 kHz to 300 GHz)," *Health physics*, vol. 118, no. 5, pp. 483–524, 2020.

[6] W. Fang *et al.*, "Safety Analysis of Long-Range and High-Power Wireless Power Transfer Using Resonant Beam," *IEEE Transactions on Signal Processing*, vol. 69, pp. 2833-2843, 2021.

## Response to Reviewer 2

*"This manuscript introduces a millimeter wave resonant beam system for SWIPT (mmRB-SWIPT), leveraging retro-directive antenna arrays to enable automatic beam alignment and enhanced transmission efficiency without additional controls. The paper presents a notable advancement in the field of SWIPT in detail and I recommend acceptance of the article."*

**Response.** We greatly appreciate your encouraging comments. Your insightful feedback has been invaluable. Thank you for your time and effort spent reviewing our submission.

R2.1 *"However, here are some questions and suggestions for authors to consider: 1.Please show the photo of the experimental setup (if available)."*

**Response.** The resonant beam system (RBS) was initially developed with an optical setup, utilizing a light beam as the spatial carrier for power transfer and information transmission. We, along with our partners, have extensively studied the optical RBS. Real-world experiments have validated the resonance mechanism and demonstrated the feasibility of power transfer, information transmission, and positioning using the optical RBS. These findings have been published in various journals [1, 2, 3, 4, 5] and conferences [6].

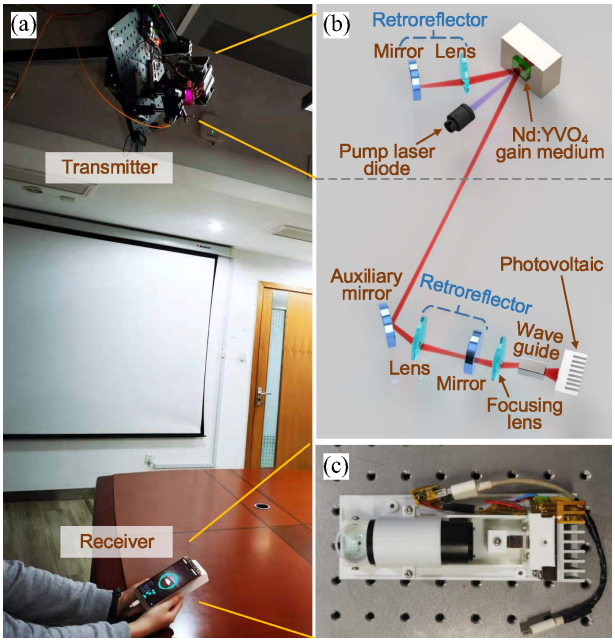


Figure R.3: Optical RBS testbed for power transfer. (a) Experiment of charging a smartphone. (b) Experimental components. (c) Receiver with the size $16.7 \times 6.0 \times 3.6\text{cm}^3$

The first experiment of the optical RBS was conducted in [1], where the resonance mechanism is validated and the power transfer capability of the system is demonstrated. Fig.R.3 depicts the testbed and the components for the system transceivers.

Further experiments were conducted to demonstrate the communication and positioning capabilities of the optical RBS. In [4], a simultaneous localization and power transfer scheme is proposed and tested. The experimental setup is shown in Fig. R.4.

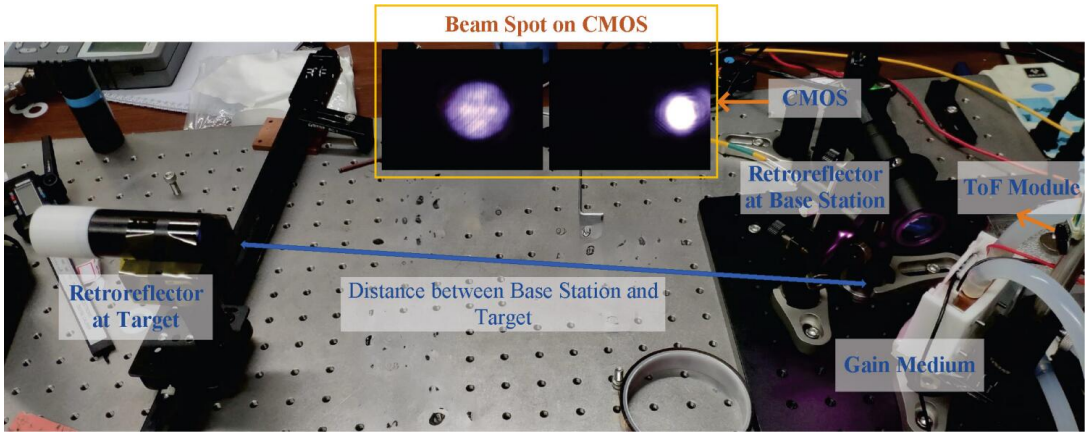


Figure R.4: Optical RBS testbed for positioning.

In the present manuscript, we propose an extension of the RBS concept into the millimeter wave (mmWave) spectrum, building upon the foundational principles of the optical RBS. While the optical and mmWave RBS share a similar resonant mechanism, this manuscript represents our first attempt to explore the mmWave RBS. Consequently, specific real-world experiments for the mmWave RBS have not yet been conducted.

We are actively planning to undertake these experiments to further validate and enhance the functionality of the mmWave RBS. The setup of the real-world experiment of mmWave RBS also resembles the one for the optical RBS. The very basic components of the optical RBS includes retro-reflectors for retro-directivity, gain medium for providing power input, and photovoltaic panel for convert optical energy to electricity. Similarly, our proposed mmWave RBS takes phase-conjugation-based retro-directive antenna array for retro-directivity, power amplifier for providing power input, and power rectifier for harvesting the received RF power. With the similar system structure and underlying principles, our previous experience with the optical RBS can be transplanted to the context of mmWave.

For now, we have included photos of the optical RBS setup to illustrate the fundamental principle, as it closely relates to our proposed mmWave RBS. We hope this provides clarity on the experimental

groundwork that supports our current work.

We appreciate your understanding and look forward to sharing the results of our upcoming experiments with you. Please follow our future publications if the RBS continues to be of research interest to you.

Thank you once again for your valuable feedback.

## References


[1] Q. Liu, M. Xiong, M. Liu, Q. Jiang, W. Fang and Y. Bai, "Charging a Smartphone Over the Air: The Resonant Beam Charging Method," *IEEE Internet of Things Journal*, vol. 9, no. 15, pp. 13876-13885, 1 Aug.1, 2022.

[2] M. Xiong, M. Liu, Q. Jiang, J. Zhou, Q. Liu and H. Deng, "Retro-Reflective Beam Communications With Spatially Separated Laser Resonator," *IEEE Transactions on Wireless Communications*, vol. 20, no. 8, pp. 4917-4928, Aug. 2021.

[3] M. Liu, S. Xia, M. Xiong, M. Xu, W. Fang and Q. Liu, "Integrated Communication and Positioning With Resonant Beam," *IEEE Transactions on Wireless Communications*, vol. 21, no. 11, pp. 9186-9199, Nov. 2022.

[4] M. Liu, Q. Jiang, Q. Liu, M. Xu, M. Xiong and W. Fang, "Simultaneous Localization and Power Transfer via Resonant Beam," *IEEE Internet of Things Journal*, vol. 10, no. 2, pp. 1414-1425, 15 Jan.15, 2023.

[5] Y. Bai, Q. Liu, L. Yang, G. B. Giannakis, W. Fang and M. Xiong, "Resonant Beam SWIPT With Telescope and Second Harmonic," *IEEE Transactions on Wireless Communications*, vol. 22, no. 7, pp. 4962-4973, July 2023.

[6] S. Han, M. Xu, M. Liu, S. Xia and Q. Liu, "Transmitter Rotation for Field of View Enhancement in Resonant Beam Wireless Power Transfer," in *2023 IEEE 24th International Workshop on Signal Processing Advances in Wireless Communications (SPAWC)*, Shanghai, China, 2023, pp. 526-530.

## Response to Reviewer 3

*"This manuscript proposed a novel simultaneous wireless information and power transfer (SWIPT) method via resonant beam system, which works on the millimeter wave frequency band. The system structure proposed assimilates the prevalent MIMO beamforming but performs better. An antenna spacing technique is introduced to separate the frequencies for downlink and uplink. The conducted experiments are solid and persuasive, particularly Fig. 12, which shows the difference between traditional beamforming technique and the proposed method. However, there are some concerns regarding this manuscript."*

**Response.** Thanks for your positive assessment of this submission. We deeply appreciate your time and effort spent on this review.

Following your suggestions, we have revised the manuscript carefully. Your itemized comments have been addressed in the revised version as follows.

R3.1 *"The authors have mentioned that the 'Resonance Beam System' was initially laser-based. What is the relationship between the laser-based RBS relate to the system proposed in this manuscript?"*

**Response.** Thank you for your valuable comments. In the manuscript, the term "Resonant Beam System" or "RBS" can be regarded as a kind of wireless system consisting of a pair of transceivers that are both equipped with retro-directive apparatus. The laser-based RBS shares some similarities with our mmWave-based RBS, yet both have their own distinctions. The similarities and distinctions can be summarized as follows:

*Similarities:*

S.1 Both of the systems rely on the principle of resonance, i.e., the signal is retro-reflected back and forth between the transceiver pair.

S.2 Both of the systems feature a self-aligning capability, i.e., the beam can be aligned adaptively without the need for extra control.

*Distinctions:*

D.1 The optical RBS takes retro-reflectors to control the light beam for resonance. Our work employs phase-conjugation antenna arrays to retro-direct the mmWave signal for resonance.

D.2 With respect to communication, the optical RBS entails complex light modulation and faces the challenge of echo interference. We proposed a dual-frequency design in this manuscript to avoid the echo interference, and the communication technique for mmWave is much easier compared with the optics.

Following your helpful comment, we have revised the Sec. I. to better explicate the advantages and challenges of the optical RBS, and to provide the readers a clearer view on the relationship between the optical RBS and the proposed mmWave RBS in this manuscript. The related paragraphs in Sec. I. are as follow, with revision highlighted in blue color, which can also be found in the revised version of our manuscript on page 1.

> The optical resonant beam system (RBS) was proposed as an effective alternative to traditional SWIPT [1, 2, 3]. By employing retro-reflectors on both the transmitter and the receiver, the lightwave can automatically follow the device's movement, realizing self-alignment. A similar structure operating at RF frequency has also been explored to provide wireless power transfer with higher efficiency [4]. The retro-reflective approach allows the system to refine the power circulating between the transmitter and the receiver, finally reaching an optimal state with a power-focused beam. However, the retro-directive beam subject the system to severe echo interference, i.e., the inbound and outbound beams interfere with each other, hindering the communication [5, 6].
>
> Millimeter wave (mmWave), recently regarded as one of the promising candidates for 6G mobile networks [7], is characterized by narrow beam transmission [8]. Despite a troublesome beam alignment [9], mmWave is potent for achieving higher power transmission efficiency and higher data rate [10]. With the resonance mechanism from the optical RBS, the beam alignment issue of mmWave can be tackled similarly.
>
> In this manuscript, we propose the millimeter wave resonant beam SWIPT system (mmRB-SWIPT) featuring higher power efficiency and obviating the need for beam alignment. Phase conjugation-based retro-directive antenna arrays are adopted to make the incoming signal retrace its way. Resembling the structure of optical RBS, we equip both the base station (BS) and the user device (UD) with retro-directive ability, enabling the beam to align automatically and follow the device inherently. A special design to separate the frequencies for downlink and uplink is introduced to address the challenge of echo interference faced by the optical RBS.

R3.2 *"The manuscript suggests that the proposed system requires the establishment of a stable resonance before providing SWIPT services. This raises questions about potential delays introduced during the resonance establishment phase. How to quantify the time required to achieve stable resonance?"*

**Response.** Thanks for your careful review, which is crucial for us to continuously improve our paper quality. The time required to setup the resonance is of great importance. We are sorry for not providing sufficient details on how to quantify it.

The required time to setup the resonance can calculated based on the propagation speed of the EM wave $c$, the required iteration in initialization $n_{\text{itr}}$, and the distance $L$ between the transceivers. For example, if the distance is 3m, and 50 iterations is required, the total time can be calculated as

$$t = \frac{2Ln_{\text{itr}}}{c} = \frac{2 \times 3 \times 50}{3 \times 10^8} = 10^{-6}\text{s} = 1\mu\text{s}.$$

The multiplication by 2 accounts for the fact that an iteration consists of two single-trip.

Following your comments, we have supplemented the analytical expressions in Sec. IV. B that can be found in blue color. In addition, numerical analysis have been conducted to determine the required time to establish the resonance, with the results depicted in Figure 8, which can be found on page 8.

> The required time to initialize the resonance is crucial for evaluating the performance of the proposed system. In particular, some application scenario may require no perceptible delay. Intuitively, the time to establish the resonance is the total distance that the EM wave needs to travel divided by the speed of it. Namely,
>
> $$t = \frac{2Ln_{\text{itr}}}{c}, \tag{3}$$
>
> where $L$ is the distance between the Tx and Rx, $n_{\text{itr}}$ is the number of iterations required to initialize, and $c$ is the speed of light. The multiplication by 2 accounts for the fact that an iteration consists of two single-trips. Thus, the delay time before the system can provide service can be determined.

R3.3 *" Since the term 'SWIPT' has already been defined in Section I, the authors should use the abbreviation immediately on page 3, beneath Fig. 4, rather than the entire term."*

**Response.** We greatly appreciate your kind and helpful comments. In accordance with your advice, we have revised the corresponding sentence in the manuscript. Specifically, the revised sentence with abbreviation can be found on page 3 in blue color. We have also carefully proof-read the manuscript and revised some sentences to better conform with the standard.

*"Overall, the manuscript is well-written, with a clear logic flow. The proposed system presents a novel and interesting SWIPT method via millimeter wave and is deserving of publication in the journal. I therefore recommend a minor revision, with the authors addressing the aforementioned concerns to enhance the manuscript's clarity and depth."*

**Response.** We would like to extend our gratitude to your positive, helpful and encouraging comments. Your time and effort spent on our work have been crucial for us to improve the quality of the manuscript.

## References


[1] M. Liu, H. Deng, Q. Liu, J. Zhou, M. Xiong, L. Yang, and G. B. Giannakis, "Simultaneous mobile information and power transfer by resonant beam," *IEEE Transactions on Signal Processing*, vol. 69, pp. 2766–2778, 2021.

[2] Y. Bai, Q. Liu, L. Yang, G. B. Giannakis, W. Fang, and M. Xiong, "Resonant beam SWIPT with telescope and second harmonic," *IEEE Transactions on Wireless Communications*, 2022.

[3] S. Xia, Q. Liu, M. Liu, W. Fang, M. Xiong, Y. Bai, and X. Li, "Auto-protection for resonant beam SWIPT in portable applications," *IEEE Internet of Things Journal*, 2023.

[4] T. Matsumuro, Y. Ishikawa, and N. Shinohara, "Basic study of both-sides retrodirective system for minimizing the leak energy in microwave power transmission," *IEICE Transactions on Electronics*, vol. 102, no. 10, pp. 659–665, 2019.

[5] M. Xiong, Q. Liu, G. Wang, G. B. Giannakis, and C. Huang, "Resonant beam communications: Principles and designs," *IEEE Communications Magazine*, vol. 57, no. 10, pp. 34–39, 2019.

[6] M. Xiong, Q. Liu, G. Wang, G. B. Giannakis, S. Zhang, J. Zhu, and C. Huang, "Resonant beam communications with echo interference elimination," *IEEE Internet of Things Journal*, vol. 8, no. 4, pp. 2875– 2885, 2020.

[7] W. Hong, Z. H. Jiang, C. Yu, D. Hou, H. Wang, C. Guo, Y. Hu, L. Kuai, Y. Yu, Z. Jiang et al., "The role of millimeter-wave technologies in 5G/6G wireless communications," *IEEE Journal of Microwaves*, vol. 1, no. 1, pp. 101–122, 2021.

[8] L. Wang, M. Elkashlan, R. W. Heath, M. Di Renzo, and K.-K. Wong, "Millimeter wave power transfer and information transmission," in *2015 IEEE Global Communications Conference (GLOBECOM)*, 2015, pp. 1–6.

[9] C. Liu, M. Li, S. V. Hanly, I. B. Collings, and P. Whiting, "Millimeter wave beam alignment: Large deviations analysis and design insights," *IEEE journal on selected areas in communications*, vol. 35, no. 7, pp. 1619–1631, 2017.

[10] L.-T. Tu and M. Di Renzo, "Analysis of millimeter wave cellular networks with simultaneous wireless information and power transfer," in *2017 International Conference on Recent Advances in Signal Processing, Telecommunications Computing (SigTelCom)*, 2017, pp. 39–43.

## Response to Reviewer 4

*"The authors proposed a transceiver architecture for SWIPT using retrodirective antenna arrays. The reviewer has the following comments."*

**Response.** Thanks for recognizing the contributions of our submission. Your time and effort dedicated to our manuscript are sincerely appreciated.

Following your suggestions, we have revised the manuscript carefully. Your comments have been addressed in the revised version as follows.

R4.1 *"The proposed SWIPT architecture is interesting. However, the analysis was performed under ideal conditions without considering practical circuit operations such as impedance matching. Additionally, the evaluation results were presented based on the aforementioned formula without incorporating circuit simulations. A discussion on the realistic performance of the proposed architecture is needed. "*

**Response.** Thank you for your positive and constructive comment. Considering practical circuit operations in our analysis is indeed of importance to strengthen our work. It would be crucial support alongside our theoretical analysis for validating the practical feasibility of the proposed system.

In our previous works on the resonant beam system (RBS), we have conducted theoretical analysis [1], circuit simulations [2], and realistic experiments [3] to fully validate the feasibility of the optical RBS. In this manuscript, we extended our optical RBS to the millimeter wave (mmWave) spectrum to address some challenges faced in the optical spectrum. The fundamental operating principles of RBS, such as resonance mechanism and energy transfer, remain consistent with the optical system. Our previous experimental validation and circuit simulations suggest that the mmWave RBS will exhibit similar behavior and feasibility.

Furthermore, while preparing this manuscript, we noticed that a work from Ryukoku University, Japan [4] has proposed a wireless power transfer (WPT) system with a similar architecture to the RBS. Particularly, they also employs retro-directive antenna on both sides of the system in attempt to increase the overall efficiency. Though different analytical models were established, a conclusion very similar to ours was reached by them, i.e., with such a retro-directive setup, the beam could be refined iteratively as it being reflected back and forth, and finally converge to a stable state with maximized efficiency. In their work, a circuit simulation was conducted with the setup shown in Fig. R.5.

Compared to our work that takes mmWave to realize SWIPT, this work aims to use microwave to achieve WPT. While the frequency spectrum and system functionality are different, their simulation

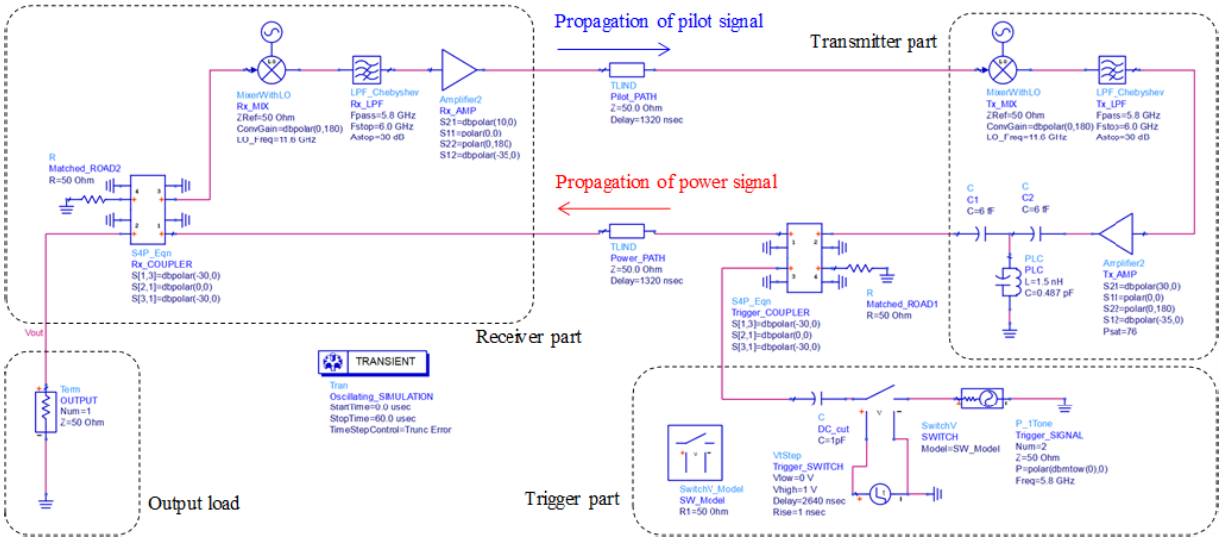


Figure R.5: The circuit simulation conducted by Ryukoku University [4].

result could also support the practical feasibility of our proposed system since the retro-directive architecture remains similar.

Consequently, the specific circuit simulation for the mmWave SWIPT system proposed in this manuscript has not yet been conducted. Following your suggestion, we have outlined this topic as a prospect for future works. We appreciate your understanding and look forward to sharing the results of our upcoming simulations and experiments with you. Please follow our future publications if the RBS continues to be of research interest to you.

R4.2 *"The explanation of the decoding process for the proposed receiver is insufficient."*

**Response.** We greatly appreciate your kind and helpful comments. In the proposed system, we adopt phase-locked-loop (PLL) to sychronize the carrier's phase and frequency. The locked carrier wave is used to perform coherent demodulation as well as to be modulated for outbound information. We apologize for not providing enough detailed explanation in our previous submission.

Following your constructive suggestion, we have added more details to explain the communication scheme of the proposed system in Sec. II., which can be found in the revised manuscript in blue color. The revision is also attached below.

### Carrier Synchronization and Modulation

In our system, as indicated in Fig. 2, the Tx array of BS and Rx array of UD (the downlink array pair) are configured to operate at $f_1$, and the Rx array of BS and Tx array of UD are configured to operate at $f_2$. After the resonance converges, the communication initiates.

To provide a synchronized phase for retro-directivity and pure carrier wave for information bearing, phase-locked loops (PLL) are employed. The processing units connected to every antenna element comprise a filter, a PLL, a low noise amplifier (LNA), and a mixer, as illustrated in Fig. 5. The locked carrier wave is also used to perform coherent demodulation to retrieve the inbound information.

The BS receives the uplink signal at $f_2$, of which the majority is directed to the PLL for synchronization. The rest of it, split by the power divider (PD), is amplified by an LNA and utilized for information demodulation. After carrier synchronization, the resulting signal from PLL is mixed with LO at $f_1+f_2$ for heterodyning. Additionally, the LO signal is pre-modulated with the downlink information. Following proper mixing and filtering, the signal is shifted to frequency $f_1$, with its phase conjugated, and carries the downlink information. Finally, the DC input is applied to amplifiers within the processing units to provide power.

For example, consider the $m$-th element on the BS side, the received uplink signal is in the form

$$\begin{aligned} u(t) =& x^{\mathrm{u}}(t)\cos(2\pi f_2 t + \varphi_m) \\ &+ y^{\mathrm{u}}(t)\sin(2\pi f_2 t + \varphi_m) \end{aligned}, \tag{4}$$

with $x^{\mathrm{u}}(t)$ and $y^{\mathrm{u}}(t)$ representing the in-phase and quadrature components of the uplink signal, respectively. For downlink information bearing, PLL recovers a pure carrier wave at frequency $f_2$

$$c(t) = \cos(2\pi f_2 t + \varphi_m), \tag{5}$$

where $\varphi_m$ is the phase term of this element. The LO signal to be mixed with is already modulated with downlink information and is in the form

$$\begin{aligned} L(t) =& x^{\mathrm{d}}(t)\cos(2\pi(f_1+f_2)t) \\ &+ y^{\mathrm{d}}(t)\sin(2\pi(f_1+f_2)t) \end{aligned}, \tag{6}$$

where $x^{\mathrm{d}}(t)$ and $y^{\mathrm{d}}(t)$ are the in-phase and quadrature components of the signal to be sent

downlink, respectively. With heterodyne, the resultant signal is

$$\begin{aligned} r(t) = &\frac{1}{2}x^{\mathrm{d}}(t)\left[\cos(2\pi f_1 t - \varphi_m) + \cos(2\pi(f_1+2f_2)t + \varphi_m)\right] \\ &+ \frac{1}{2}y^{\mathrm{d}}(t)\left[\sin(2\pi f_1 t - \varphi_m) + \sin(2\pi(f_1+2f_2)t + \varphi_m)\right] \end{aligned}. \tag{7}$$

The signal centered at frequency $f_1+2f_2$ can be easily removed with bandpass filter. The final signal entering the $m$-th antenna element is

$$\begin{aligned} d(t) = &x^{\mathrm{d}}(t)\cos(2\pi f_1 t - \varphi_m) \\ &+ y^{\mathrm{d}}(t)\sin(2\pi f_1 t - \varphi_m) \end{aligned}. \tag{8}$$

Comparing (4) with (8), we can see that $d(t)$ is phase-conjugated version of $u(t)$ and modulated with downlink information.

On the UD side, the arriving signal at $f_1$ is divided into three parts after filtering: the majority is harvested for charging power output, a small portion is used for demodulating the received information, and an extremely small fraction is routed to the PLL for phase recovery. The similar approach to phase conjugation and modulation also applies on the UD side, the output of PLL is then mixed with modulated LO at $f_1+f_2$ to provide a phase-conjugated and information-bearing signal.

We would also like to respectfully highlight that the primary contribution of this manuscript is to propose a SWIPT system architecture featuring self-adaptive beam alignment. Regarding the information transmission, the underlying communication channel is very close to conventional mmWave wireless channels. The similarity ensures that well-established encoding and decoding processes universally adopted in mmWave systems are also applicable to our system.

R4.3 *"Some equations are unclear:*

*1) In equation (5), this criterion for azimuth and elevation angles in URA were not considered.*

*2) In equation (10), it seems to describe rectifying each antenna unit. However, rectifying after passing through the combiner obtained in the previous iteration may result in higher energy harvesting performance."*

**Response.** Thank you so much for your comment. Your in-depth feedback is crucial for us to improve the academic quality of our work. In accordance to your comments, we have the following explanation and revision:

1) The equation (5) was derived in the scenario of uniform linear array (ULA) to intuitively present how does the spacing arrangement ensures retro-directivity. We have revised the related paragraphs and supplemented the derivation process for uniform rectangular array (URA) which needs to consider the azimuth and elevation angles. The supplemented information in Sec. II. are as follows, which can also be found in the revised version of our revised manuscript in blue color.

To maintain the retro-directivity with altered frequency $f_2$, the goal is to make the transmitting angle $\theta_2$ equal to the incident angle $\theta_1$. We have:

$$\begin{cases} \theta_1 = \arccos\left(\dfrac{\Delta\varphi_1}{2\pi}\dfrac{\lambda_1}{d_1}\right) \\ \theta_2 = \arccos\left(\dfrac{\Delta\varphi_2}{2\pi}\dfrac{\lambda_2}{d_2}\right) \end{cases}. \tag{9}$$

Hence, by ensuring that the spacing between adjacent antenna units is proportional to the respective frequencies, i.e., $\lambda_1/d_1 = \lambda_2/d_2$, we will have $\theta_1 = \theta_2$, thus maintaining the retro-directivity with different Tx and Rx frequencies [5].

This spacing arrangement remains applicable to uniform rectangular array (URA) employed in the proposed system. Consider a URA whose the spacing in the $x$-direction is $d_{x1}$ and in the $y$-direction is $d_{y1}$. The phase difference between adjacent elements in the $x$-direction and the $y$-direction can be calculated as

$$\begin{cases} \Delta\varphi_{x1} = \dfrac{2\pi d_{x1}}{\lambda_1}\sin\theta_1\cos\phi_1 \\ \Delta\varphi_{y1} = \dfrac{2\pi d_{y1}}{\lambda_1}\sin\theta_1\sin\phi_1 \end{cases}, \tag{10}$$

where $\theta_1$ and $\phi_1$ are the elevation and azimuth angle of the incoming wave at frequency $f_1$.

For the outgoing wave to have the same azimuth angle $\phi_2 = \phi_1$ and elevation angle $\theta_2 = \theta_1$ at frequency $f_2$, we require:

$$\begin{cases} \Delta\varphi_{x2} = \dfrac{2\pi d_{x2}}{\lambda_2}\sin\theta_2\cos\phi_2 \\ \qquad\quad = -\dfrac{2\pi d_{x1}}{\lambda_1}\sin\theta_1\cos\phi_1 = -\Delta\varphi_{x1} \\ \Delta\varphi_{y2} = \dfrac{2\pi d_{y2}}{\lambda_2}\sin\theta_2\sin\phi_2 \\ \qquad\quad = -\dfrac{2\pi d_{y1}}{\lambda_1}\sin\theta_1\sin\phi_1 = -\Delta\varphi_{y1} \end{cases}. \tag{11}$$

Since we have $\lambda_1 \neq \lambda_2$, the spacing for the URA at frequency $f_2$ must satisfy

$$\frac{\lambda_1}{\lambda_2} = \frac{d_{x1}}{d_{x2}} = \frac{d_{y1}}{d_{y2}}, \tag{12}$$

where $d_{x2}$ is the spacing for the $x$-direction and $d_{y2}$ is for the $y$-direction.

2) Yes, in equation (10), we consider each antenna unit individually and take the summation of them to obtain the total power received. This approach is adopted from [6], in which the authors proposed a calculation method for the received power with antenna arrays. The highlight of the method adopted is that it is applicable if the distance is in the far-field region of a **single antenna element**, regardless of whether or not it is in the far-field region of the array antenna.

We found this approach particularly suitable for our work since the main application scenario of the system we proposed is indoors, where the typical transmission distance lies between 1m to 10m. The range satisfies the far-field requirement for a single antenna element, while lies in the near-field if the array is considered as a whole. The adopted approach allows us to calculate the received power within this distance with only far-field scenario is considered.

Following your suggestion, we have revised the manuscript to better explicate this idea. The revision regarding this issue can be found in Sec. III. A. in blue color, and is also attached below.

Considering there are $M$ Tx units, the total power received by the $n$-th Rx antenna can be calculated by summing the contributions from all $M$ units. That is:

$$\begin{aligned} P_{\mathrm{R}_n} &= \frac{4\pi}{2\mu c}\left|\sum_{m=1}^{M} |\mathbf{r}_{mn}|\mathbf{E}_{mn}\right|^2 \\ &= \frac{\lambda^2}{16\pi^2}\left|\sum_{m=1}^{M} \frac{\sqrt{P_{\mathrm{T}_m} G_{\mathrm{T}_{mn}} G_{\mathrm{R}_{mn}}}}{|\mathbf{r}_{mn}|} e^{-j(k\mathbf{r}_{mn}-\varphi_m)}\right|^2, \end{aligned} \tag{13}$$

where each $m$-th Tx antenna element is considered individually.

Finally, the power received by the Rx array with a total of $N$ antenna elements can be calculated by summing the power received by each Rx antenna element as

$$\begin{aligned} P_{\mathrm{R}} &= \sum_{n=1}^{N} P_{\mathrm{R}_n} \\ &= \frac{\lambda^2}{16\pi^2}\sum_{n=1}^{N}\left|\sum_{m=1}^{M} \frac{\sqrt{P_{\mathrm{T}_m} G_{\mathrm{T}_{mn}} G_{\mathrm{R}_{mn}}}}{|\mathbf{r}_{mn}|} e^{-j(k\mathbf{r}_{mn}-\varphi_m)}\right|^2. \end{aligned} \tag{14}$$

In the above derivation, the total received power by the antenna array is calculated by taking summation on each antenna element. Since the power relationship is based on the gain of the single antenna element, the far-field requirement applies to the size of the single antenna element, not the antenna array [6]. Suppose the transmission distance is $L$, the largest dimension of a single antenna element is $D_{\text{ele}}$, and the one of the antenna array is $D_{\text{arr}}$. In instances where $D_{\text{ele}}^2/\lambda \ll L \ll D_{\text{arr}}^2/\lambda$, the approach remains applicable.

R4.4 *"A discussion on the effectiveness in multi-device scenarios is needed. In particular, how should the power allocation problem be solved?"*

**Response.** We greatly appreciate your kind and helpful comments. The proposed system is expected to have the capability for multi-device operation [7, 8]. We apologize for not providing adequate information refarding this topic. Following your constructive suggestion, we have added description of multiple access scheme in our revised manuscript. You can find the supplemented information in Sec. II. of the revised version of our manuscript in blue color. The discussion is also attached below.

### Multiple Access

The resonance mechanism allows the BS to establish resonance with multiple UDs simultaneously [7, 8], making it possible to provide SWIPT service to multiple users with only one BS. However, due to the possibly unknown UD-BS relative location, the signal from each UD needs to be processed individually and exclusively to realize the retro-directivity thus maintaining the stable resonance. To this end, time division multiple access (TDMA) can be adopted. Upon receiving pilot signals from more than one UDs, the BS can formulate frame-based scheduling scheme to allow multiple access.

Consider the transmission from BS as a series of frames. Each frame is composed of $n+1$ time slots given the number of users $n$. During the time slot designated to the $i$-th user, the BS will only process the signal from it and disregard all other signals. Also, after being assigned to specific time slot, the UD should be idle during others' time slot to avoid possible interference. In the last time slot of each time frame, the BS is configured to listen for request to initialize link from other possible users. Despite the complexity, this TDMA implementation not only allows the BS to provide service to multiple users simultaneously, but also reduces the possible interference.

The power allocation is primarily based on the scheduling algorithm adopted by BS, which

may vary depending on the specific need of the application scenario. For example, in a smart home scenario, computers may have access to more time slots and/or with longer duration while time slots for home accessories may be shorter. More sophisticated scheduling techniques can be explored to better conform to the specific application scenario.

The power allocation problem for multi-device scenario can be formulated as an optimization problem. It can be modelled as a game where each device aims to optimize its own utility. Techniques like Nash Equilibrium can be used to find stable power allocation strategies. While we believe the power allocation is worthy of future research, the complexity due to the interactions between devices and the varying conditions of the communication channels may be beyond the scope of this manuscript. In our previous works, the scheduling and optimization problem have been studied in the context of optical RBS [7, 8, 9]. We hope these reference could provide clarity on the power allocation problem of the RBS. Future works on the optimization of the system proposed in this manuscript are also on our research agenda.

We greatly appreciate your valuable feedback and your understanding.

R4.5 *"There are some comments regarding the experimental results:*

*1) The system model assumed the far field, but the experiment was conducted in the near field area.*

*2) How was the required time calculated?*

*3) The physical values for the beam gain are missing in Figures 9, 12, and 15."*

**Response.** Thank you so much for your comment. Your meticulous examination has been invaluable for us to enhance the quality of our manuscript. Following your comments, we have made the following explanation and revision:

1) Thank you for your meticulous comment. In this manuscript, the analytical models were based on the assumption of far field. The distances adopted in our experiments also conforms to the far field requirement if we consider the dimension of single antenna unit.

We proposed a millimeter wave-based resonant beam system to provide SWIPT service. The main application scenario of this system is expected to be indoors, where the typical transmission distance lies between 1m to 10m. The far-field region requires that $L > 2D^2/\lambda$, where $L$, $D$, and $\lambda$ denote the transmission distance, the largest dimension of the antenna, and the wavelength. In our case, transmission distance indeed falls short for the far field criterion if the antenna array is considered as a whole.

To address this issue, we followed an analysis approach proposed in [6], which has been adopted and recognized in various peer-reviewed publications [10, 11, 12]. By considering each antenna element individually and taking the summation of every element, this approach allow us to conduct numerical analysis in the near-field region of the array antenna given the far-field condition for a single antenna element is met.

We regret that we fail to provide enough detail on this point and therefore caused confusion to you. Following your comment, we have made revision regarding this issue in Sec. III. A in blue color.

Considering there are $M$ Tx units, the total power received by the $n$-th Rx antenna can be calculated by summing the contributions from all $M$ units. That is:

$$\begin{aligned} P_{\mathrm{R}_n} &= \frac{4\pi}{2\mu c}\left|\sum_{m=1}^{M}|\mathbf{r}_{mn}|\mathbf{E}_{mn}\right|^2 \\ &= \frac{\lambda^2}{16\pi^2}\left|\sum_{m=1}^{M}\frac{\sqrt{P_{\mathrm{T}_m}G_{\mathrm{T}_{mn}}G_{\mathrm{R}_{mn}}}}{|\mathbf{r}_{mn}|}e^{-j(k\mathbf{r}_{mn}-\varphi_m)}\right|^2, \end{aligned} \tag{15}$$

where each $m$-th Tx antenna element is considered individually.

Finally, the power received by the Rx array with a total of $N$ antenna elements can be calculated by summing the power received by each Rx antenna element as

$$\begin{aligned} P_{\mathrm{R}} &= \sum_{n=1}^{N} P_{\mathrm{R}_n} \\ &= \frac{\lambda^2}{16\pi^2}\sum_{n=1}^{N}\left|\sum_{m=1}^{M}\frac{\sqrt{P_{\mathrm{T}_m}G_{\mathrm{T}_{mn}}G_{\mathrm{R}_{mn}}}}{|\mathbf{r}_{mn}|}e^{-j(k\mathbf{r}_{mn}-\varphi_m)}\right|^2. \end{aligned} \tag{16}$$

In the above derivation, the total received power by the antenna array is calculated by taking summation on each antenna element. Since the power relationship is based on the gain of the single antenna element, the far-field requirement applies to the size of the single antenna element, not the antenna array [6]. Suppose the transmission distance is $L$, the largest dimension of a single antenna element is $D_{\mathrm{ele}}$, and the one of the antenna array is $D_{\mathrm{arr}}$. In instances where $D_{\mathrm{ele}}^2/\lambda \ll L \ll D_{\mathrm{arr}}^2/\lambda$, the approach remains applicable.

2) The required time to setup the resonance is calculated based on the propagation speed of the EM wave $c$, the required iteration in initialization $n_{\mathrm{itr}}$, and the distance $L$ between the transceivers. For example, if the distance is 3m, and 50 iterations is required, the total time can be calculated

as:

$$t = \frac{2Ln_{\text{itr}}}{c} = \frac{2 \times 3 \times 50}{3 \times 10^8} = 10^{-6}\text{s} = 1\mu\text{s}.$$

The multiplication by 2 accounts for the fact that an iteration consists of two single-trips.

To better explicate the details regarding the required time, we have added a paragraph along with analytical expressions in Sec. IV. B. We are sorry for the confusion caused by the missing information. The supplemented information can be found in Sec. IV. B in blue color. In addition, numerical analysis have been conducted to determine the required time to establish the resonance, with the results depicted in Figure 8, which can be found on page 8.

> The required time to initialize the resonance is crucial for evaluating the performance of the proposed system. In particular, some application scenario may require no perceptible delay. Intuitively, the time to establish the resonance is the total distance that the EM wave needs to travel divided by the speed of it. Namely,
>
> $$t = \frac{2Ln_{\text{itr}}}{c}, \tag{17}$$
>
> where $L$ is the distance between the Tx and Rx, $n_{\text{itr}}$ is the number of iterations required to initialize, and $c$ is the speed of light. The multiplication by 2 accounts for the fact that an iteration consists of two single-trips. Thus, the delay time before the system can provide service can be determined.

3) Thank you for your helpful comment. We have added the physical values in the above mentioned figures. To enhance the readability, we have also made some minor modifications to the figures. The revised figures can be found on page 9, 10, and 11 respectively with their captions highlighted in blue color. For your convenience, the modified figures are also attached in the end of the response.

R4.6 *"There are minor comments:*

*1) p. 3., l. 4, Reference missing.*

*2) p. 3., l. 1, p. 6., l. 41, Do not start a sentence with 'I.e."'*

**Response.** Thank you so much for your comment. Your meticulous examination of our submission is of great importance for us to improve the quality of this manuscript. We have revised this sentence according to your suggestion as follows:

1) The reference [13, 14, 15] have been added to provide readers with a view of the mentioned method.

2) We have reformed the sentences to make sure "i.e." does not lead a sentence.

We have also carefully proof-read the manuscript and revised some sentences to better explicate our ideas. The revised sentences can be found in the revised version of this manuscript in blue color.

We would like to express our gratitude again for your time and effort spent reviewing our submission. Your suggestions have been very helpful for us to improve our work.

## References


[1] M. Liu *et al.*, "Simultaneous Mobile Information and Power Transfer by Resonant Beam," *IEEE Transactions on Signal Processing*, vol. 69, pp. 2766-2778, 2021.

[2] J. Zhou, M. Xiong, M. Liu, Q. Liu and S. Zhou, "Transient Analysis for Resonant Beam Charging and Communication," *IEEE Internet of Things Journal*, vol. 9, no. 4, pp. 3074-3082, 15 Feb.15, 2022.

[3] Q. Liu, M. Xiong, M. Liu, Q. Jiang, W. Fang and Y. Bai, "Charging a Smartphone Over the Air: The Resonant Beam Charging Method," *IEEE Internet of Things Journal*, vol. 9, no. 15, pp. 13876-13885, 1 Aug.1, 2022.

[4] T. Matsumuro, Y. Ishikawa, and N. Shinohara, "Basic study of both-sides retrodirective system for minimizing the leak energy in microwave power transmission," *IEICE Transactions on Electronics*, vol. 102, no. 10, pp. 659–665, 2019.

[5] Y. Kang, X. Q. Lin, Y. Li and B. Wang, "Dual-Frequency Retrodirective Antenna Array With Wide Dynamic Range for Wireless Power Transfer," *IEEE Antennas and Wireless Propagation Letters*, vol. 22, no. 2, pp. 427-431, Feb. 2023.

[6] C. M. Song *et al.*, "Analysis of Received Power in RF Wireless Power Transfer System With Array Antennas," *IEEE Access*, vol. 9, pp. 76315-76324, 2021.

[7] M. Liu, G. Wang, G. B. Giannakis, M. Xiong, Q. Liu and H. Deng, "Wireless Power Transmitter Deployment for Balancing Fairness and Charging Service Quality," *IEEE Internet of Things Journal*, vol. 7, no. 3, pp. 2223-2234, March 2020.

[8] W. Fang, G. Wang, G. B. Giannakis, Q. Liu, X. Wang and H. Deng, "Channel-Dependent Scheduling in Wireless Energy Transfer for Mobile Devices," *IEEE Transactions on Vehicular Technology*, vol. 69, no. 3, pp. 3330-3340, March 2020.

[9] W. Fang, Q. Zhang, M. Liu, Q. Liu, and P. Xia, "Earning maximization with quality of charging service guarantee for iot devices," *IEEE Internet of Things Journal*, vol. 6, no. 1, pp. 1114–1124, Aug. 2019.

[10] X. Wu *et al.*, "Accurate and Efficient Method for Analyzing the Transfer Efficiency of Metasurface-Based Wireless Power Transfer System," *IEEE Transactions on Antennas and Propagation*, vol. 71, no. 1, pp. 783-795, Jan. 2023.

[11] Y. Zeng, S. Chen, Y. Cui, J. Yang and Y. Fu, "Joint Resource Allocation and Trajectory Optimization in UAV-Enabled Wirelessly Powered MEC for Large Area," *IEEE Internet of Things Journal*, vol. 10, no. 17, pp. 15705-15722, 1 Sept.1, 2023.

[12] K. F. Warnick, F. Broyde, L. Jelinek, M. Capek and E. Clavelier, "Generalized Friis Transmission Formula Using Active Antenna Available Power and Unnamed Power Gain," *IEEE Transactions on Antennas and Propagation, Early Access*, 2024.

[13] X. Wang, S. Sha, J. He, L. Guo, and M. Lu, "Wireless power delivery to low-power mobile devices based on retro-reflective beamforming," *IEEE Antennas and Wireless Propagation Letters*, vol. 13, pp. 919–922, 2014.

[14] H. Koo, J. Bae, W. Choi, H. Oh, H. Lim, J. Lee, C. Song, K. Lee, K. Hwang, and Y. Yang, "Retroreflective transceiver array using a novel calibration method based on optimum phase searching," *IEEE Transactions on Industrial Electronics*, vol. 68, no. 3, pp. 2510–2520, 2021.

[15] Y. Jiang, B. Liu, W. Li, B. Zhu, J. Cao, and X. Wang, "Retro-reflective Beamforming to Multiple Targets Based on Time-reversal for Microwave Power Transmission," in *2022 IEEE MTT-S International Wireless Symposium (IWS)*, vol. 1, pp. 1-3, IEEE, 2022.

## Revised Figures

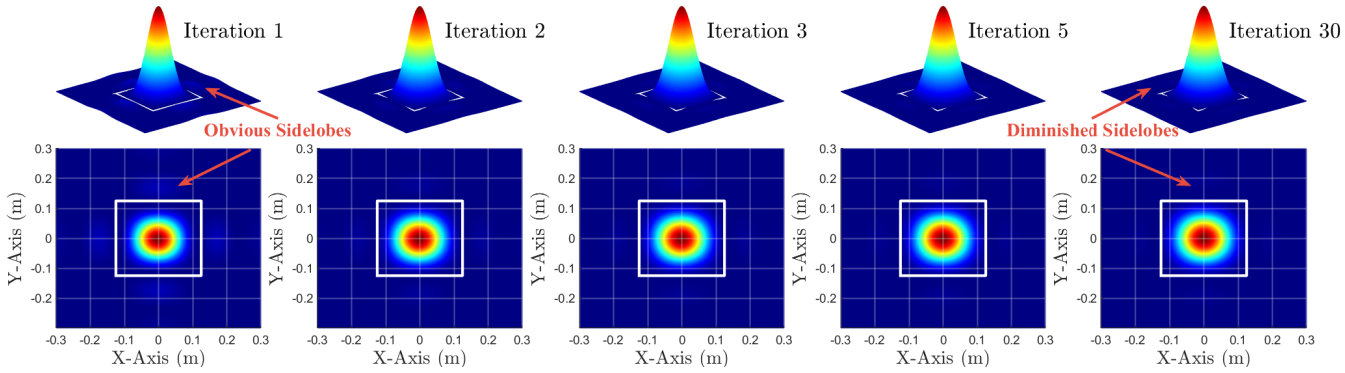


Figure R.6: Revised version of Figure 9.

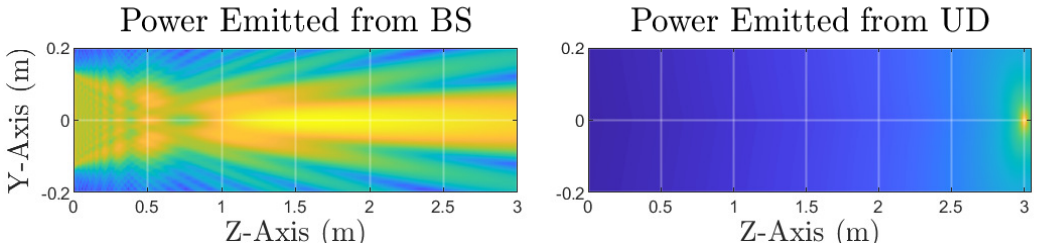


(a) Retro-directive beamforming

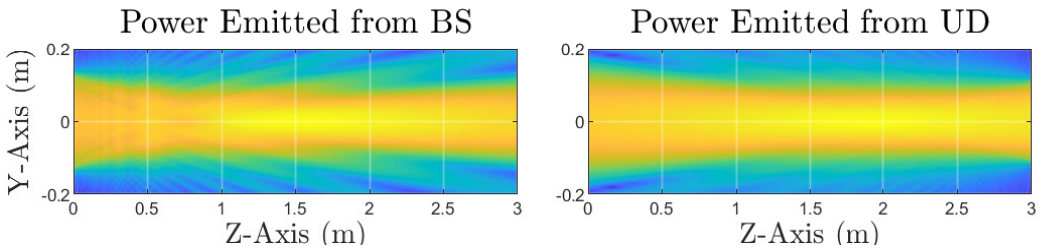


(b) RBS

Figure R.7: Revised version of Figure 10.

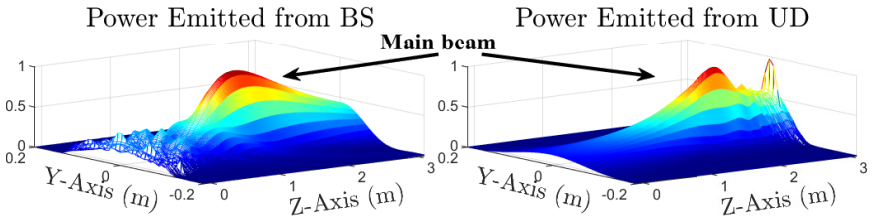


(a) $\sigma_\phi^2 = 0$

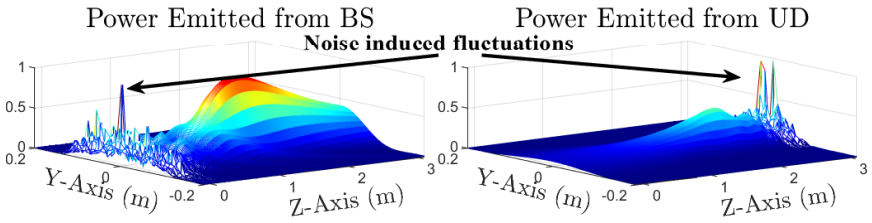


(b) $\sigma_\phi^2 = 310.17$

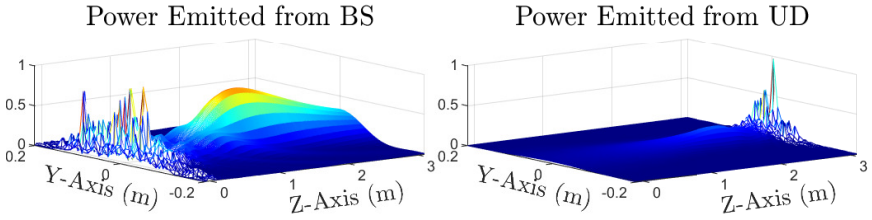


(c) $\sigma_\phi^2 = 500$

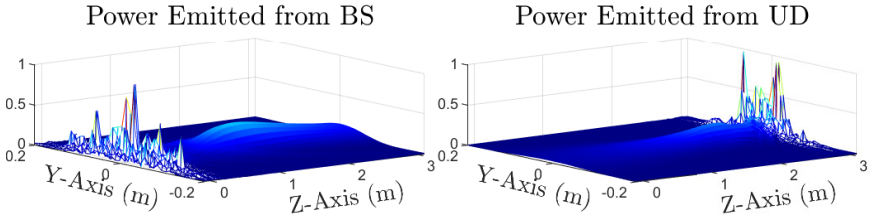


(d) $\sigma_\phi^2 = 800$

Figure R.8: Revised version of Figure 12.